

# Synthesis and crystal structure of decamethyl-1,4-diphospha-2,3,5,6,7-pentasilabicyclo[2.2.1]heptane and crystal structure of dodecamethyl-1,4-diphospha-2,3,5,6,7,8-hexasilabicyclo[2.2.2]octane

Gerlinde M. Kollegger <sup>a</sup>, Ulrike Katzenbeisser <sup>a</sup>, Karl Hassler <sup>a,\*</sup>, Carl Krüger <sup>b</sup>,  
David Brauer <sup>c</sup>, Ralf Gielen <sup>c</sup>

<sup>a</sup> Institut für Anorganische Chemie der T.U., Stremayrgasse 16, A-8010 Graz, Austria

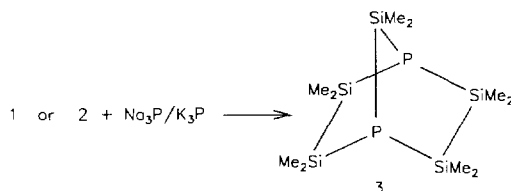
<sup>b</sup> Max Planck Institut für Kohleforschung, Postfach 011325, Kaiser Wilhelm Platz 1, D-4300 Mülheim / Ruhr, Germany

<sup>c</sup> Institut für Anorganische Chemie, Bergische Universität-Gesamthochschule, Gausstrasse 20, D-42097 Wuppertal, Germany

Received 28 November 1996; revised 9 January 1997

## Abstract

The reaction of 1,2-dichlorotetramethyldisilane **1** as well as tri(chlorodimethylsilyl)methylsilane **2** with sodium potassium phosphide (prepared from the elements in dimethoxyethane) affords decamethyl-1,4-diphospha-2,3,5,6,7-pentasilabicyclo[2.2.1]heptane, **3**.



With **1**, dodecamethyl-1,4-diphospha-2,3,5,6,7,8-octasilabicyclo[2.2.2]octane, **4** is also formed. **3** was characterized by <sup>29</sup>Si- and <sup>31</sup>P – NMR spectroscopy, elemental analysis, infrared and Raman spectroscopy. The crystal structures of **3** and **4** have been elucidated by X-ray crystallography. © 1997 Elsevier Science S.A.

## 1. Introduction

Quite a number of rings and cages consisting of an alternating arrangement of P and Si atoms have been described in the literature. The reaction which has been used most frequently for the preparation of these compounds is the salt elimination from a phosphide and a silicon halide, usually a silicon chloride. In all these cases, organic groups R and R' such as methyl, ethyl, *tert*-butyl or phenyl have been used as exocyclic substituents.

A selection of previously prepared structures is presented in Scheme 1.

Another method that has been introduced successfully is the reaction of disilenes or phosphasilenes with white phosphorus P<sub>4</sub>. Large organic substituents such as 2,4,6-trimethylphenyl or 2,4,6-triisopropylphenyl are mandatory to stabilize SiSi or SiP double bonds.

Not many rings and cages containing SiSi bonds have been described so far (Scheme 2). Again organic substituents had to be used to stabilize the PSi skeletons, and all were prepared by the salt elimination reaction. At this time, no cyclic or polycyclic silylphosphanes are known which bear hydrogen substituents exclusively.

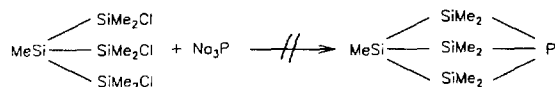
Cage-like silylphosphanes with the phosphorus atoms surrounded by three Si atoms (the former acting as a bridging atom) can be prepared by the reaction of sodium potassium phosphide [16] with multiply func-

\* Corresponding author.

tional silanes. If disilanes or oligosilanes are used, cages like 1,4-diphospha-2,3,5,6,7,8-hexasilabicyclo[2.2.2]octane [14] or 1-phospha-2,3,4,5,6,7,8-heptasilabicyclo[2.2.2]octane [15] are formed (Scheme 2, lower right).

## 2. Syntheses

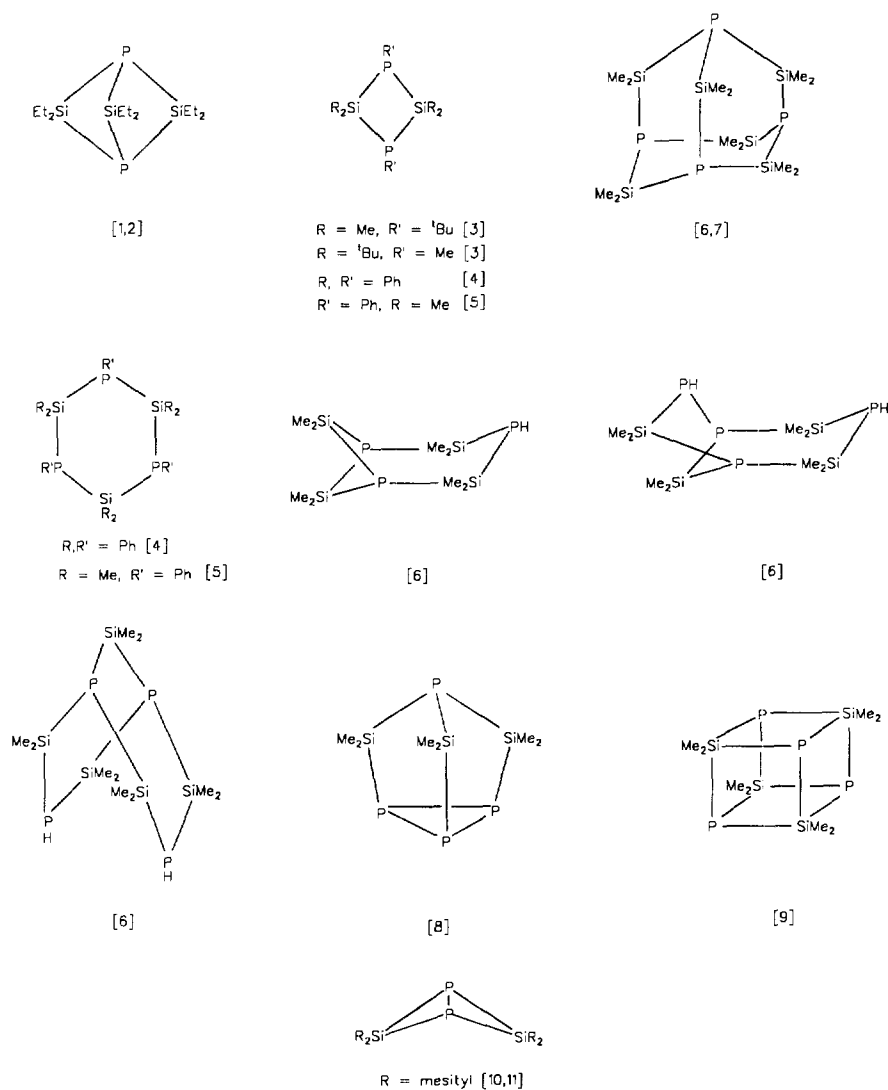
In an unsuccessful attempt to prepare 1-phospha-2,3,4,5-tetrasilabicyclo[1.1.1]pentane from  $\text{Na}_3\text{P}/\text{K}_3\text{P}$  and  $\text{MeSi}(\text{SiMe}_2\text{Cl})_3$ , **2**, in DME



we were able to isolate 1,4-diphospha-2,3,5,6,7-penta-

silabicyclo[2.2.1]heptane **3** in 11% yield. Obviously, the  $\text{Si}_4$  skeleton of **2** is broken down completely in this reaction, and the  $\text{SiMe}_2$  groups are used for the formation of **3**. A tentative reaction mechanism involves a stepwise cleavage of the  $\text{SiSi}$  bonds by  $\text{Na}_3\text{P}/\text{K}_3\text{P}$  as well as metal halogen exchange reactions that are responsible for the formation of  $\text{SiSi}$  bonds and of cyclosilanes such as dodecamethylcyclohexasilane and decamethylcyclopentasilane. As a side reaction, DME is attacked by the resulting silanides.

We have therefore re-examined the reaction of  $\text{Na}_3\text{P}/\text{K}_3\text{P}$  [16] with 1,2-dichlorotetramethyldisilane **1**, expecting an  $\text{SiSi}$  bond cleavage to occur simultaneously with  $\text{SiP}$  bond formation, which would lead to cages other than bicyclo[2.2.2]octanes. When the reaction is carried out in DME, the title compound **3** and the



Scheme 1. Examples of silicon phosphorus rings and cages with alternating P-Si backbone [1–11].

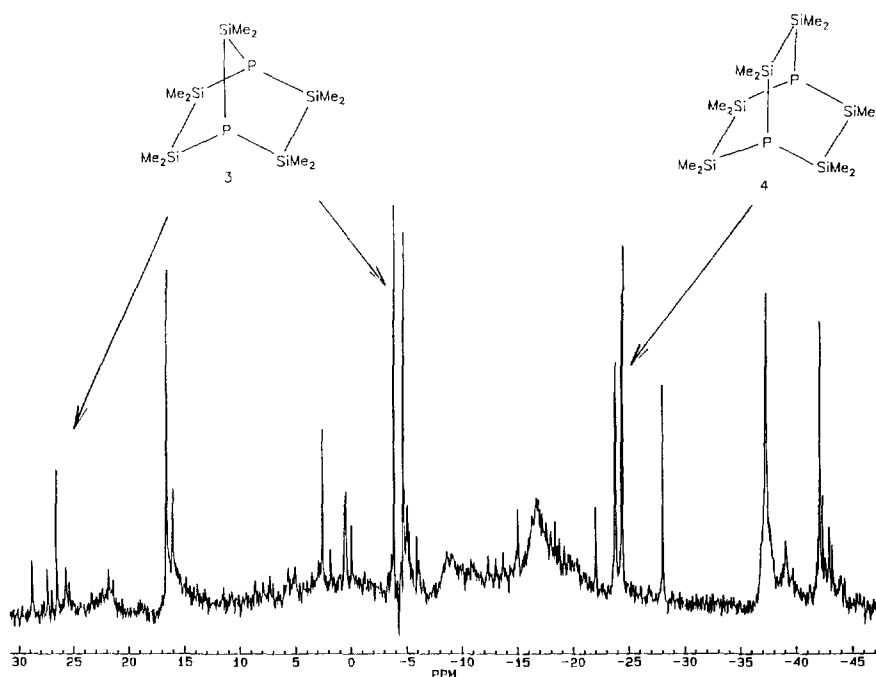
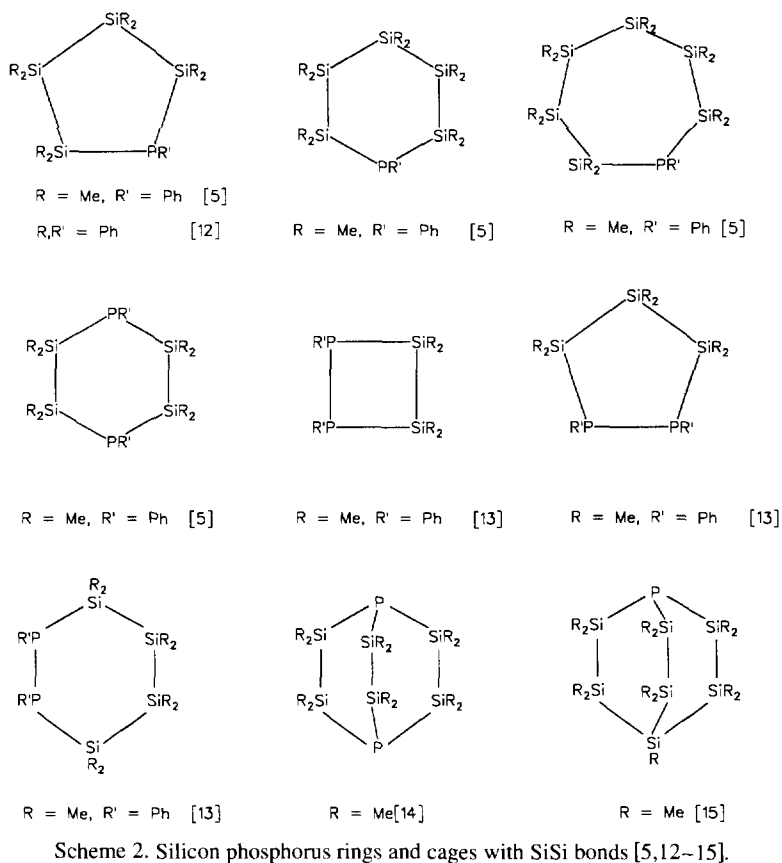


Fig. 1.  $^{29}\text{Si}$  NMR spectrum of the products formed in the reaction between  $\text{Me}_2\text{ClSiSiCIME}_2$  and  $\text{Na}_3\text{P}/\text{K}_3\text{P}$ .

bicyclo[2.2.2]octane **4** form in a ratio of approximately 1:1.

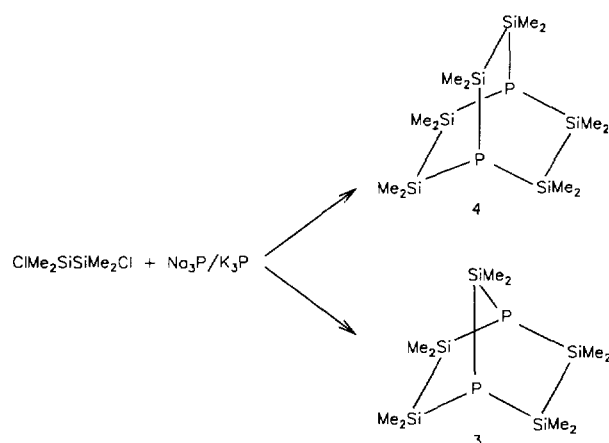


Fig. 1 presents the  $^{29}\text{Si}$  NMR spectrum of the reaction mixture. The signals with multiplicities caused by  $^{29}\text{Si}^{31}\text{P}$  coupling originate from the cages **3** and **4**, while those at  $-42.1$  ppm and at  $-42.4$  ppm result from  $\text{Si}_6\text{Me}_{12}$  and  $\text{Si}_5\text{Me}_{10}$  respectively.

### 3. Description of the crystal structures

#### 3.1. Structure of **3**

Crystals of **3** are composed of discrete molecules, the two present in the asymmetric unit being depicted in Fig. 2. Their structures are roughly compliant with  $C_{2v}$  symmetry, although the small variations of chemically equivalent bond distances and angles (Tables 1 and 2), in particular the lengths of the Si–Si and Si–P bonds, are statistically significant; thus we will refer to the average structural parameters in the following.

The constraints of the bicyclic structure dictate that the five- and six-membered rings of **3** assume envelope

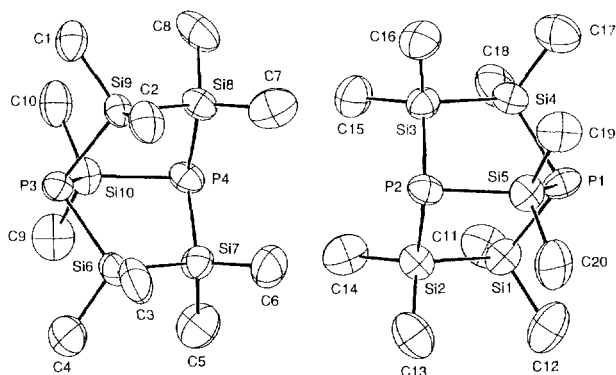


Fig. 2. Perspective drawings of the two independent molecules of **3** with hydrogen atoms removed for clarity.

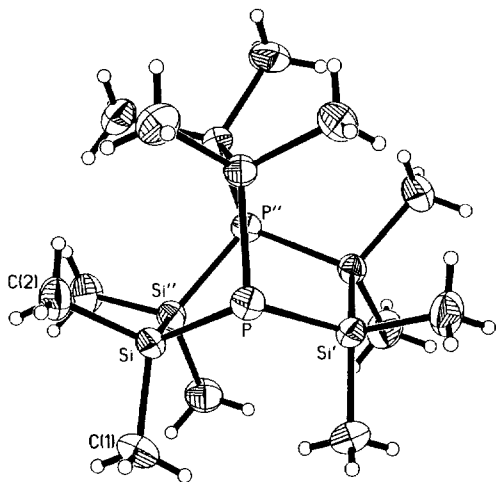
Table 1  
Selected bond distances (Å) in **3**

P(1)–Si(1)	2.254(1)	P(3)–Si(6)	2.253(1)
P(1)–Si(4)	2.259(1)	P(3)–Si(9)	2.263(1)
P(1)–Si(5)	2.260(1)	P(3)–Si(10)	2.267(1)
P(2)–Si(2)	2.258(1)	P(4)–Si(7)	2.257(1)
P(2)–Si(3)	2.264(1)	P(4)–Si(8)	2.256(1)
P(2)–Si(5)	2.262(1)	P(4)–Si(10)	2.265(1)
Si(1)–Si(2)	2.378(1)	Si(6)–Si(7)	2.357(1)
Si(3)–Si(4)	2.349(1)	Si(8)–Si(9)	2.352(1)
Si(1)–C(11)	1.861(5)	Si(6)–C(3)	1.874(4)
Si(1)–C(12)	1.864(5)	Si(6)–C(4)	1.868(4)
Si(2)–C(13)	1.873(4)	Si(7)–C(5)	1.864(4)
Si(2)–C(14)	1.872(4)	Si(7)–C(6)	1.861(4)
Si(3)–C(15)	1.880(4)	Si(8)–C(7)	1.860(4)
Si(3)–C(16)	1.869(4)	Si(8)–C(8)	1.861(4)
Si(4)–C(17)	1.871(4)	Si(9)–C(1)	1.868(4)
Si(4)–C(18)	1.865(5)	Si(9)–C(2)	1.874(4)
Si(5)–C(19)	1.865(4)	Si(10)–C(9)	1.867(4)
Si(5)–C(20)	1.864(5)	Si(10)–C(10)	1.864(4)

and boat conformations respectively. The average P–Si bond distance in the six-membered rings, 2.258(4) Å, is not significantly longer than that reported for

Table 2  
Selected bond angles (deg) in **3**

Si(1)–P(1)–Si(4)	104.1(1)	Si(6)–P(3)–Si(9)	103.4(1)
Si(1)–P(1)–Si(5)	94.2(1)	Si(6)–P(3)–Si(10)	93.5(1)
Si(4)–P(1)–Si(5)	93.6(1)	Si(9)–P(3)–Si(10)	93.6(1)
Si(2)–P(2)–Si(3)	103.5(1)	Si(7)–P(4)–Si(8)	103.1(1)
Si(2)–P(2)–Si(5)	93.7(1)	Si(7)–P(4)–Si(10)	93.9(1)
Si(3)–P(2)–Si(5)	93.5(1)	Si(8)–P(4)–Si(10)	93.3(1)
P(1)–Si(1)–Si(2)	107.2(1)	P(3)–Si(6)–Si(7)	107.3(1)
P(2)–Si(2)–Si(1)	107.1(1)	P(4)–Si(7)–Si(6)	107.8(1)
P(2)–Si(3)–Si(4)	107.9(1)	P(4)–Si(8)–Si(9)	107.6(1)
P(1)–Si(4)–Si(3)	107.0(1)	P(3)–Si(9)–Si(8)	107.6(1)
P(1)–Si(5)–P(2)	110.2(1)	P(3)–Si(10)–P(4)	110.2(1)
P(1)–Si(1)–C(11)	113.0(1)	P(3)–Si(6)–C(3)	112.7(1)
P(1)–Si(1)–C(12)	106.4(2)	P(3)–Si(6)–C(4)	107.6(1)
P(2)–Si(2)–C(13)	106.9(2)	P(4)–Si(7)–C(5)	106.3(2)
P(2)–Si(2)–C(14)	112.4(1)	P(4)–Si(7)–C(6)	113.7(1)
P(2)–Si(3)–C(15)	112.5(1)	P(4)–Si(8)–C(7)	112.4(1)
P(2)–Si(3)–C(16)	106.6(1)	P(4)–Si(8)–C(8)	106.5(2)
P(1)–Si(4)–C(17)	107.2(1)	P(3)–Si(9)–C(1)	106.5(1)
P(1)–Si(4)–C(18)	112.4(1)	P(3)–Si(9)–C(2)	113.2(1)
P(1)–Si(5)–C(19)	110.0(1)	P(3)–Si(10)–C(9)	110.7(1)
P(1)–Si(5)–C(20)	110.3(2)	P(3)–Si(10)–C(10)	109.8(1)
P(2)–Si(5)–C(19)	110.4(1)	P(4)–Si(10)–C(9)	110.0(1)
P(2)–Si(5)–C(20)	110.2(1)	P(4)–Si(10)–C(10)	110.2(1)
Si(2)–Si(1)–C(11)	112.8(1)	Si(7)–Si(6)–C(3)	112.9(1)
Si(2)–Si(1)–C(12)	111.2(2)	Si(7)–Si(6)–C(4)	111.1(1)
Si(1)–Si(2)–C(13)	111.2(1)	Si(6)–Si(7)–C(5)	110.8(2)
Si(1)–Si(2)–C(14)	112.6(1)	Si(6)–Si(7)–C(6)	111.3(2)
Si(4)–Si(3)–C(15)	111.9(1)	Si(9)–Si(8)–C(7)	112.0(1)
Si(4)–Si(3)–C(16)	110.8(1)	Si(9)–Si(8)–C(8)	111.4(1)
Si(3)–Si(4)–C(17)	110.1(1)	Si(8)–Si(9)–C(1)	112.3(1)
Si(3)–Si(4)–C(18)	113.7(1)	Si(8)–Si(9)–C(2)	110.5(1)
C(11)–Si(1)–C(12)	106.2(2)	C(3)–Si(6)–C(4)	105.2(2)
C(13)–Si(2)–C(14)	106.5(2)	C(5)–Si(7)–C(6)	106.8(2)
C(15)–Si(3)–C(16)	107.0(2)	C(7)–Si(8)–C(8)	106.8(2)
C(17)–Si(4)–C(18)	106.2(2)	C(1)–Si(9)–C(2)	106.7(2)
C(19)–Si(5)–C(20)	105.6(2)	C(9)–Si(10)–C(10)	105.8(2)

Fig. 3. A perspective drawing of **4**.

(PhPSi<sub>2</sub>Me<sub>4</sub>)<sub>2</sub>, 2.252 Å, which adopts a chair conformation [17]. The latter possesses P–Si–Si (105.0(2)°) and Si–P–Si (104.4(1)°) bond angles which vary little from the corresponding values (107.4(3)° and 103.5(4)°) in the six-membered ring of **3**. The average Si–P–Si angle in the five-membered ring of **3**, 93.7(3)°, is much smaller.

As is apparent in Fig. 2, the methyl substituents of the six-membered ring occupy either axial or equatorial positions. This differentiation has little significance for the Si–Si–C bond angles, the values for the two sets of angles averaging 112.2(10)° and 111.1(6)° respectively. On the contrary, the average P–Si–C (axial) angle, 112.8(5)°, is clearly larger than the average P–Si–C (equatorial) angle, 106.8(4)°.

### 3.2. Structure of **4**

A drawing of **4** is presented in Fig. 3, and important structural parameters are gathered in Table 3. In the solid state, each molecule occupies a site of crystallographic *D*<sub>3</sub> symmetry with the P-atoms on the threefold axis and each twofold axis bisecting an Si–Si bond. Thus, unlike the eclipsed conformation that would be

Table 3  
Selected bond distances (Å), bond angles (deg) and torsion angles (deg) in **4**<sup>a</sup>

P–Si	2.2576(5)	Si–C(1)	1.873(2)
Si–Si <sup>ii</sup>	2.3590(7)	Si–C(2)	1.876(2)
Si–P–Si <sup>i</sup>	101.49(2)	C(1)–Si–Si <sup>ii</sup>	109.34(7)
P–Si–Si <sup>ii</sup>	115.07(2)	C(2)–Si–Si <sup>ii</sup>	109.58(7)
P–Si–C(1)	108.18(7)	C(1)–Si–C(2)	105.73(9)
P–Si–C(2)	108.53(7)		
P–Si–Si <sup>ii</sup> –P <sup>ii</sup>	–21.99(4)	Si <sup>i</sup> –P–Si–Si <sup>ii</sup>	–40.83(3)
C(1)–Si–Si <sup>ii</sup> –C(2) <sup>ii</sup>	–21.35(10)	Si <sup>iii</sup> –P–Si–Si <sup>ii</sup>	63.57(3)

<sup>a</sup> Symmetry code: (i) –y, x–y, z; (ii) x–y, –y, 0.5–z; (iii) –x+y, –x, z.

required for the –SiMe<sub>2</sub>–SiMe<sub>2</sub>– fragments by *D*<sub>3h</sub> symmetry, a non-eclipsed conformation is allowed in the crystal, and indeed the corresponding torsion angles (Table 3) open up some 21°. However, the opening of these nine torsion angles per molecule has its price; for instance, six torsion angles like Si<sup>i</sup>–P–Si–Si<sup>ii</sup>, which would have ideal 60° values under *D*<sub>3h</sub> symmetry, are closed by 19.17(3)°. This payoff of torsional strain should ensure that the potential barrier for a *D*<sub>3</sub> → *D*<sub>3h</sub> rearrangement of the free molecule will be low. A similar situation was described for [2.2.2]bicyclooctane [18] and its 1,4-diaza analogue [19]. Thus the latter exhibits torsions about its –CH<sub>2</sub>–CH<sub>2</sub>– bonds which are about half as large as the analogous values found for **4** and a barrier at the *D*<sub>3h</sub> structure of only 100 cm<sup>–1</sup>. The reasonably low thermal parameters found for **4** indicate that its structure is not dynamic in the crystal. Presumably the large displacements of the methyl groups required by an equilibrating structure are prohibited by packing forces, which may also help determine the extent of distortion from *D*<sub>3h</sub> symmetry in the solid state.

The six-membered rings of **4** are in the skew-boat form with P–Si and Si–Si bond lengths which are metrically identical to the corresponding average distances in the six-membered ring of **3**. The Si–P–Si (101.49(2)°) and P–Si–Si (115.07(2)°) bond angles in **4** are respectively 2.0(4)° smaller and 7.7(3)° larger than

Table 4  
Infrared and Raman spectra (cm<sup>–1</sup>) and calculated normal vibrations of **3**

IR (s)	Ra (s)	Vibration	A <sub>1</sub> , calc.	A <sub>2</sub> , calc.	B <sub>1</sub> , calc.	B <sub>2</sub> , calc.
835vs,b	838vw	ρCH <sub>3</sub>	838	838	844	836
800vs,b	800w	ρCH <sub>3</sub>	779	777	777	783
763s	770vw	ρCH <sub>3</sub>	754	754	758	754
730s		ν <sub>as</sub> SiC <sub>2</sub>	730	725	725	720
		ν <sub>as</sub> SiC <sub>2</sub>				712
688s	683mw	ν <sub>s</sub> SiC <sub>2</sub>			681	
661vs	671m	ν <sub>s</sub> SiC <sub>2</sub>	662	664		668
650shm		ν <sub>s</sub> SiC <sub>2</sub>	661			
	637w					
483vs	495vw	νPSi			502	511
465sh	463w	νSiSi	475			
456vs		νSih			444	
	439w	νPSi		446		
412w	415w	impurity				
390s	383mw	νPSi				390
379s		νPSi	388			
348vw	343vs	νPSi	328			
	275w	δSiC		260	271	
	255mw	δSiC	252	242	243	253
	233w	δSiC	232	214	210	
	194vs	δSiC				191
	159sh	δSiC	168	154		163
	145s	δSiC	142	147	151	148
	133ms	δSiC	131			120
		δcage	118	116	184	50
		δcage	11	12	12	

the corresponding average valency angles in the six-membered ring of **3**. With an additional SiMe<sub>2</sub> entity in the bicyclic system, the intramolecular P...P separation in **4**, 4.3428(5) Å, is much larger than the average value for **3**, 3.713(6) Å.

#### 4. Vibrational spectra of **3**

Table 4 lists the infrared and Raman vibrational frequencies of decamethyl-1,4-diphospha-2,3,5,6,7-heptasilabicyclo[2.2.1]heptane as well as the results of a normal coordinate analysis which was performed using the FG-method [20]. The experimental geometry has been used for the calculation of the G-matrix. Symmetry coordinates have been calculated employing C<sub>2v</sub> symmetry, and a simplified local symmetry force field for the SiMe<sub>2</sub> groups, as described in Ref. [21] for H<sub>3</sub>SiSiMe<sub>2</sub>SiH<sub>3</sub>, has been introduced. SiSi and SiP valence force constants have been taken from normal coordinate calculations of P(SiMe<sub>3</sub>)<sub>3</sub> [22], Si<sub>6</sub>Me<sub>12</sub> [23] and P(SiMe<sub>2</sub>SiMe<sub>2</sub>)<sub>3</sub>P [14] without further refinement. The reasonable agreement between the calculated normal vibrations of the cage (Table 4) and the experimental values justifies the simple force field given in Table 5.

#### 5. Experimental details

##### 5.1. X-ray crystal structure determinations

Crystals of **3** and **4** were obtained by crystallization from *n*-hexane and by vacuum sublimation at 60 °C respectively. Both were mounted in glass capillaries under argon. X-ray data were collected with a CAD4 diffractometer. While one unique quadrant of reflections was measured for **3**, a hemisphere of data was collected for **4**. The scope of the latter data set allowed us to develop the structure not only in the trigonal but also in the monoclinic and triclinic crystal systems and thus address questions pertaining to space group ambiguity. Since the data for **3** were collected with Mo Kα radi-

Table 5  
Local symmetry force field (Ncm<sup>-1</sup>) of the SiMe<sub>2</sub>-groups in **3**<sup>a</sup>

$\nu_s$ SiC <sub>2</sub>	2.80	0.1	0	0	0	0
$\delta$ SiC <sub>2</sub>		0.20	0	0	0	0
$\nu_{as}$ SiC <sub>2</sub>			2.70	0	0	0
$\gamma$ SiC <sub>2</sub>				0.15	0	0
$\rho$ SiC <sub>2</sub>					0.15	0
$\tau$ SiC <sub>2</sub>						0.15

<sup>a</sup> Non-zero interaction force constants with SiP and SiSi stretching coordinates were:  $F(\nu_s$ SiP<sub>2</sub> or  $\nu_s$ PSi<sub>2</sub>/ $\nu_s$ SiC<sub>2</sub>) = 0.10;  $F(\nu$ SiSi/ $\nu_s$ SiC<sub>2</sub>) = 0.10;  $F(\nu_s$ SiP<sub>2</sub> or  $\nu_s$ PSi<sub>2</sub>/ $\delta$ SiC<sub>2</sub>) = -0.10;  $F(\nu$ SiSi/ $\delta$ SiC<sub>2</sub>) = -0.10.

Table 6  
Crystal data for **3** and **4**

	<b>3</b>	<b>4</b>
Formula	C <sub>10</sub> H <sub>30</sub> P <sub>2</sub> Si <sub>5</sub>	C <sub>12</sub> H <sub>36</sub> P <sub>2</sub> Si <sub>6</sub>
MW	352.7	410.9
Space group	C2/c	R $\bar{3}c$
<i>a</i> (Å)	18.409(5)	9.6928(9)
<i>b</i> (Å)	22.014(4)	9.6928(9)
<i>c</i> (Å)	20.653(3)	44.206(3)
$\alpha$ (deg)	90	90
$\beta$ (deg)	95.67(1)	90
$\gamma$ (deg)	90	120
Z	16	6
<i>D</i> <sub>c</sub> (g cm <sup>-3</sup> )	1.13	1.14
<i>t</i> (°C)	20	21
$\lambda$ (Å)	0.71069	1.54178
2 $\theta$ max (deg)	55	150
Measured reflections	10078	5243
Unique reflections	9522	830
Observed ( <i>F</i> > 4 $\sigma$ ( <i>F</i> ))	6217	800
Crystal size (mm <sup>3</sup> )	0.46 × 0.63 × 0.42	0.21 × 0.22 × 0.26
$\mu_\lambda$ (mm <sup>-1</sup> )	0.472	4.45
Transmission		0.3076–0.5413
<i>R</i> <sup>a</sup>	0.051	0.031
<i>wR</i>	0.055 <sup>b</sup>	0.082 <sup>c</sup>
$\Delta\rho$ (max) (e Å <sup>-3</sup> )	0.40	0.37
Parameters	307	36

<sup>a</sup> All residuals are summed over just the observed reflections.

<sup>b</sup>  $wR = [\sum[w(F_o - F_c)^2]/\sum[wF_o^2]]^{1/2}$ .

<sup>c</sup>  $wR = \{\sum[w(F_o^2 - F_c^2)^2]/\sum[w(F_o^2)^2]\}^{1/2}$ .

tion, no absorption correction was necessary; but the data for **4**, which were measured with Cu Kα radiation, were corrected for absorption. Crystal data and refinement details are given in Table 6.

The structures were solved by direct methods and refined with all non-hydrogen atoms anisotropic. For **3** the hydrogen atoms were included assuming staggered conformations for the Si–C bonds. For **4** each set of methyl hydrogen atoms was treated as a rigid group for which the torsional coordinate about the associated Si–C bond was optimized [24]; however, no significant deviations from staggered geometries were found. Since structural solution and refinement in the space groups  $P\bar{1}$ , C2/c and R $\bar{3}c$  all led to essentially identical structural parameters, we will only report the results in R $\bar{3}c$ . A few violations of the systematic absences required by this space group were detected, but Weissenberg photographs made after data collection revealed that the data crystal was contaminated by a small, secondary scatterer. Furthermore, models developed in the lower-symmetry space groups neither accounted for the anomalous intensities nor yielded lower residuals. (Additional crystallographic details may be obtained from Fachinformationszentrum Karlsruhe, Gesellschaft für wissenschaftliche Information mbH, D-76344 Eggenstein-Leopoldshafen by quoting the deposit num-

ber CSD-XXXXX for **3** and CSD-406404 for **4**, the authors and the literature reference.)

### 5.2. Techniques

All operations have been carried out under a nitrogen atmosphere. Silicon halogen and silicon phosphorus bonds are highly sensitive to moisture, and SiP bonds are readily attacked by oxygen. Therefore, all solvents have been distilled from potassium and saturated with dry nitrogen.

Sodium potassium phosphide are highly flammable when exposed to air and must be handled very carefully.

C,H analyses have been carried out on a Heraeus Micro U apparatus with tolerances of  $\pm 0.3\%$  for C and  $\pm 0.25\%$  for H.

IR spectra have been recorded as paraffinic suspensions held between CsBr plates. Raman spectra of the crystalline solids have been measured with a Spex Ramalog with excitation from an He–Ne laser (6328 Å, 50 mW).

GC/MS spectra have been recorded using an HP gas chromatograph HP 5890-II coupled to an HP 5971 mass spectrometer. Polymethylsiloxane columns with a length of 25 m and a diameter of 0.32 mm have been used.

### 5.3. Synthesis of $P_2(\text{SiMe}_2)_5$ from $\text{MeSi}(\text{SiMe}_2\text{Cl})_3$ and $\text{Na}_3/\text{K}_3\text{P}$

To a suspension of sodium potassium phosphide in 200 ml of DME, prepared from 3.5 g (113 mmol) of  $\text{P}_4$  and 3.76 g (113 mmol) of sodium–potassium alloy (1:3 weight ratio) was added dropwise a solution of 12.2 g (37.7 mmol) of  $\text{MeSi}(\text{SiMe}_2\text{Cl})_3$  [25] in 50 ml of DME. Reflux was maintained during this operation, and was continued for 7 h after complete addition of the silane. The salts were then removed by filtration. After evaporation of the solvent in vacuo 50 ml of heptane were added. The solution was refluxed for a short time and decanted from the remaining salts. The yellowish, oily residue obtained after removal of the solvent was fractionated in vacuo. At 135 °C and 0.1 mbar, 1.2 g (11%) of pure, colourless  $\text{P}_2(\text{SiMe}_2)_5$  deposited in the condenser and was recrystallized from *n*-hexane.

Surprisingly, the cage can be analysed without decomposition by gas chromatography coupled with mass spectrometry, using a polysiloxane column.  $\text{C}_{10}\text{H}_{30}\text{Si}_5\text{P}_2$  (exp./calc.) C 34.26/34.11, H 8.35/8.58%. The  $^{29}\text{Si}$  NMR spectrum consists of a triplet for the Si-atom which is bonded to two P-atoms ( $\delta(\text{Si}) = +26.6$  ppm relative to TMS,  $^1J(\text{SiP}) = 50.8$  Hz) as well as of a pseudo-doublet at  $-4.3$  ppm with an effective coupling constant of 51.7 Hz for the Si atoms within the six-membered ring.

### 5.4. Synthesis of $\text{P}_2(\text{SiMe}_2)_5$ from $\text{Me}_2\text{ClSiSiClMe}_2$ and $\text{Na}_3/\text{K}_3\text{P}$

A suspension of sodium potassium phosphide  $\text{Na}_3/\text{K}_3\text{P}$  in 1000 ml of DME was prepared from 12.3 g (400 mmol) of  $\text{P}_4$ , 20.3 g (882.6 mmol) Na and 16 g (410.3 mmol) K as described in the literature [16]. The excess of sodium and potassium was removed by amalgamation, and 112.2 g (600.0 mmol) of  $\text{Me}_2\text{ClSiSiClMe}_2$  dissolved in 300 ml of DME was added dropwise. The reaction mixture warmed up immediately, and the addition was carried out at such a rate that the reflux was maintained. After completion, the salts were removed by filtration and the volume of the filtrate was reduced to ca. 200 ml. Crystallization at  $-30^\circ\text{C}$  afforded 20–25 g of  $\text{P}(\text{SiMe}_2\text{SiMe}_2)_3\text{P}$  which was separated by filtration.

The solvent was removed from the filtrate by evaporation in vacuo, and the yellow viscous residue was fractionated. 20–25 g of  $\text{P}_2(\text{SiMe}_2)_5$  were collected in the temperature range between 120 and 140 °C/0.05 mbar and purified by crystallization from *n*-hexane

### Acknowledgements

Financial support of the 'Fonds zur Förderung der wissenschaftlichen Forschung', Vienna (project No. P 8204-CHE) is gratefully acknowledged.

### References

- [1] G.W. Parshall, R.V. Lindsey, J. Am. Chem. Soc. 81 (1959) 6273.
- [2] G. Fritz, P. Amann, Z. Anorg. Allg. Chem. 535 (1986) 106.
- [3] G. Fritz, R. Uhlmann, Z. Anorg. Allg. Chem. 442 (1978) 95.
- [4] H. Schumann, H. Benda, Chem. Ber. 104 (1971) 333.
- [5] R.T. Oakley, D.A. Stanislawski, R. West, J. Organomet. Chem. 157 (1978) 389.
- [6] G. Fritz, R. Biastoch, Z. Anorg. Allg. Chem. 535 (1986) 63.
- [7] G. Fritz, R. Uhlmann, W. Hölderich, Z. Anorg. Allg. Chem. 442 (1987) 168.
- [8] G. Fritz, R. Uhlmann, Z. Anorg. Allg. Chem. 440 (1978) 168.
- [9] M. Baudler, G. Scholz, K.F. Tebbe, M. Feher, Angew. Chem. 101 (1989) 352.
- [10] M. Drieß, A.D. Fanta, D. Powell, R. West, Angew. Chem. 101 (1989) 1087.
- [11] M. Drieß, H. Pritzkow, M. Reisgys, Chem. Ber. 9 (1991) 124.
- [12] E. Hengge, U. Brychcy, Monatsh. Chem. 97 (1966) 1309.
- [13] T.H. Newman, J.C. Calabrese, R.T. Oakley, D.A. Stanislawski, R. West, J. Organomet. Chem. 225 (1982) 211.
- [14] K. Hassler, J. Organomet. Chem. 246 (1983) C31.
- [15] K. Hassler, G.M. Kollegger, H. Siegl, C. Kratky, J. Organomet. Chem. in press.
- [16] G. Becker, W. Hölderich, Chem. Ber. 108 (1975) 2484.
- [17] A.W. Cordes, P.F. Schubert, R.T. Oakley, Can. J. Chem. 57 (1979) 174.

- [18] O. Ermer, J.D. Dunitz, *Helv. Chim. Acta* 52 (1969) 1861.
- [19] A. Yokozeki, K. Kuchitsu, *Bull. Chem. Soc. Jpn.* 44 (1971) 72.
- [20] E.B. Wilson Jr., J.C. Decius, P.C. Cross, *Molecular Vibrations*, McGraw-Hill, New York, 1955.
- [21] K. Schenzel, K. Hassler, *Spectrochim. Acta Part A*: 52 (1996) 637.
- [22] K. Hassler, *Monatsh. Chem.*, 115 (1984) 713.
- [23] K. Hassler, *Spectrochim. Acta Part A*: 37 (1981) 541.
- [24] G.M. Sheldrick, *SHELXTL PC Version 5.0: An Integrated System for Solving, Refining and Displaying Crystal Structures from Diffraction Data*, Siemens Analytical X-ray Instruments Inc., 1994.
- [25] K. Hassler, *Monatsh. Chem.* 117 (1986) 613.